MOLEKUL
eISSN: 2503-0310

Articles
https://doi.org/10.20884/1.jm.2024.19.2.11105

The Role of The Ni/HZSM-5 Ratio on The Anisole Hydrodeoxygenation Reaction

Khoirina Dwi Nugrahaningtyas[1]*, I F Nurcahyo[1], Yuniawan Hidayat[1], Fitria Rahmawati[1], Zaki Fadlulloh[1], Eddy Heraldy[1], Nisriina 'Abidah Qurrotul'aini[2]

[1]Chemistry Department, Sebelas Maret University, Faculty of Mathematics and Natural Sciences, Surakarta 57126, Indonesia
[2]Department of Chemical Engineering, Faculty of Engineering, Universitas Gadjah Mada, Sleman, Yogyakarta 55284, Indonesia

*Corresponding author email: khoirinadwi@staff.uns.ac.id

Received February 02, 2024; **Accepted** April 30, 2024; **Available online** July 20, 2024

ABSTRACT. Bio-oil is a renewable energy source with high oxygen levels, and anisole is a chemical widely employed in research to represent it. Catalytic hydrodeoxygenation (HDO) reduces the oxygen content. A catalyst known as nickel-modified HZSM-5 has shown promising results for HDO. Meanwhile, catalyst efficiency depends on the Ni/HZSM-5 ratio. So, this study aims to determine how the Ni/HZSM-5 ratio influences the catalyst's properties, activity, and selectivity in anisole HDO. The Ni/HZSM-5 catalyst was made using the wet impregnation method with various ratios of Ni/HZSM-5. The catalysts were analyzed for their morphology using scanning electron microscopy-energy-dispersive X-ray (SEM-EDX). The diffraction patterns were studied using X-ray diffraction (XRD). Surface area and porosity were determined through gas sorption analysis (GSA). Then, the acidity strength was evaluated via temperature-programmed ammonia desorption (NH_3-TPD). The characterization results show Ni was successfully impregnated and distributed evenly in HZSM-5 without changing the primary structure. Adding Ni metal to HZSM-5 increases the surface area of the catalyst but reduces its acid strength. The catalytic performance of the catalysts was then evaluated in a flow reactor at 400 °C, using 15 mL/min H_2 gas. The liquid products of the reaction were analyzed using gas chromatography-mass spectroscopy (GC-MS). The results of the catalytic performance show that $Ni_{4.5}$/HZSM-5 has the highest catalytic activity in anisole conversion. At the same time, $Ni_{6.4}$/HZSM-5 shows the highest selectivity towards benzene-toluene-xylene (BTX).

Keywords: Hydrodeoxygenation, nickel, anisole, heterogeneous catalyst, acidity.

INTRODUCTION

Bio-oil is an alternative renewable energy derived from the pyrolysis of biomass. As a fuel, bio-oil needs improvement through, among others, the HDO method, which can remove the oxygen contained therein. Since its structure has a high complexity, anisole which has a simpler structure but is still similar to the bio-oil structure needs to be taken as an approach. Catalysts play an important role in the HDO reaction because they provide active sites in vacancies, active metals, Bronsted acid sites, or Lewis acids, which can activate oxygenated groups belonging to the target compound (He & Wang, 2012; Rogers & Zheng, 2016).

Metal-based catalysts, often first transition metals like Ni, are required for the HDO process. The HDO reaction necessitates metal-based catalysts, often first transition metals such as Ni. Triggers based on nickel are relatively affordable and have strong catalytic activity (Jin et al., 2014). Furthermore, Ni can activate hydrogen and strongly block polymerization hydrocarbons in the HDO process (Li et al., 2017). Metal-support catalysts are commonly used in catalysis to increase surface area and prevent deactivation (Botas et al., 2012; Zhang et al., 2018). One of the excellent supports is zeolite due to its large surface area, high heat resistance, selective pores, large adsorption capacity, and acidity that can be controlled (Buzetzki et al., 2011; Rahimi & Karimzadeh, 2011; Zhang et al., 2018)(Buzetzki et al., 2009; Rahimi & Karimzadeh, 2011; J. Zhang et al., 2018). The presence of support is particularly crucial in enhancing conversion in the HDO process because it contains Bronsted acid sites that can activate oxygen groups (He & Wang, 2012; Venkatesan et al., 2021; Zhang et al., 2019). H-Zeolite Socony Mobile-5 (HZSM-5) is a popular zeolite due to its high thermal stability, acidity, and selectivity (Li et al., 2020). Our previous study also demonstrated that HZSM-5 type zeolite has the highest activity and selectivity for HDO anisole compared to mordenite and Indonesian-activated natural zeolite (Nugrahaningtyas et al., 2024).

Ni metal on HZSM-5 primarily produces methyl cyclopentane and cyclohexane. These products show an aromatic ring saturation pathway after the initial hydrogenation of benzene (Li et al., 2020). The metal-

support ratio affects the selectivity and conversion of the hydrodeoxygenation reaction. Several researchers have varied the catalyst preparation, including the metal-support ratio (Zhang et al., 2018; Ranga et al., 2019). The research found that the selectivity rises with increasing metal loading, but the conversion decreases. Jin and coworkers reported a 53% benzene selectivity in their HDO reaction, carried out in a batch reactor under H_2 of 3.0 MPa and a nickel-support ratio of 10% (Jin et al., 2014). Meanwhile, other researchers obtained a 100% anisole conversion and a 70% cyclohexane selectivity when they conducted the HDO reaction in a flow reactor with H_2 gas and a 20% nickel-support ratio(Yang et al., 2014).

Researchers used nitrogen as a carrier gas in a flow reactor and adjusted the nickel-HZSM-5 metal ratio by 0.5%, 1%, or 5%. They found that a 5% nickel-ZSM-5 catalyst had the highest BTX selectivity at 98.7%, with a yield of 4.3%. Meanwhile, a 0.5% nickel-HZSM-5 catalyst yielded the highest at 33.8% in the HDO anisole reaction. In another study, a 5% Ni/USY catalyst resulted in a cyclohexane selectivity and yield of 82.6% and 61%, respectively, in a batch reactor under hydrogen pressure(Gamliel et al., 2018; J. Zhang et al., 2018).

In the present work, we have investigated the effect of the Ni/ZSM-5 ratio on catalyst characteristics and HDO performance. The Ni/HZSM-5 catalyst was created through the wet impregnation method. Catalyst performance was tested in the HDO of anisole using a fixed-bed reactor under an H_2 flow rate of 15 mL/minute and a reaction temperature of 400 °C. We have successfully identified correlations between catalyst properties, such as morphology, metal phase, diffraction pattern, texture, and acidity, based on their metal ratio, and the activity and selectivity of HDO.

EXPERIMENTAL SECTION

Materials and Instrumentation

The materials used in this study were HZSM-5 ACS Material (Si/Al ratio = 26), $Ni(NO_3)_2.6H_2O$ (p.a Merck), 25% NH_3 (p.a Merck), anisole (p.a Merck Germany without purification). Nitrogen and Hydrogen gas were acquired from PT SAMATOR, Indonesia. The prepared catalyst was then characterized with SEM-EDX (FEI Inspect S-50-Ametex), XRD (Rigaku Miniflex), GSA (NOVA 1200e) and NH_3-TPD (Micromeritics, USA).

Preparation of catalysts.

According to our previous work, the Ni/ZSM-5 catalyst was produced utilizing the wet impregnation approach (Mazlan et al., 2022; Nugrahaningtyas et al., 2022; Nugrahaningtyas et al., 2022(1)). The catalyst was prepared by loading 1.6 mol of $Ni(NO_3)_2.6H_2O$ into 20 grams of HZSM-5. The subsequent procedure entails adding double-distilled water to HZSM-5 until the solution volume reaches 200 mL. The mixture is then refluxed at 30°C for 16 hours, followed by a temperature increase to 80°C for an additional 4 hours. Finally, the mixture is evaporated with a rotary evaporator until it becomes powder.

The powder activation was carried out by calcination and reduction procedures. In the calcination process, the Ni/HZSM-5 catalyst is heated at a temperature of 550 °C for 4 hours, and N_2 gas is supplied at a rate of 15 mL/minute at a pressure of 1 atmosphere. The next step is reduction by heating at a temperature of 400 °C for 2 hours under H_2 gas at a 10 mL/minute flow rate. The catalyst obtained is called $Ni_{1.6}$/HZSM-5. The same process was carried out to obtain $Ni_{4.5}$/HZSM-5 and $Ni_{6.4}$/HZSM-5 catalysts. The catalysts were analyzed using various equipment in a series of analyses. Morphological and metal dispersion studies were performed using SEM-EDX, XRD, GSA, and NH_3-TPD.

The samples were analyzed using SEM to examine their morphology. The results were presented as images that showed the differences in HZSM-5 before and after combining it with Ni metal. These images revealed the presence of Ni metal on the surface of HZSM-5. Element mapping was used to determine the distribution of Ni metal on the surface, and the metal content was determined based on EDX data.

Analysis of diffraction patterns obtained by XRD. The data show certain 2θ peaks from samples of HZSM-5 and Ni/HZSM-5. The diffractogram pattern of the catalyst was compared to various ICSD standards using Rietica software and the Le Bail technique (Nugrahaningtyas et al., 2022; Sabiilagusti et al., 2021; Tamer, 2013; Toraya, 2016; Will, 2006). The ICSD standards that used were: #61010 for HZSM-5, ICSD #53807 for Ni, and ICSD #24014 for NiO. The closeness of the Rp (residual percentage) and Rwp (residual weight percentage) values to zero indicates the suitability of the diffractogram pattern to the standard used. This match determines the type of metal phase present in the catalyst. The molar weight percentage has been calculated using an equation based on previous research results(Will, 2006).

$$w_p = \frac{S_p(ZMV)_p}{\left(\sum_j S_j(ZMV)_j / \tau_j\right)\tau_p}$$

The formula for the relative weight fraction of phase p in a mixture of j phases is represented by wp. In the refinement process, S, Z, M, and V are the Rietveld scale factors. Z represents the number of formula units per unit cell, mass of the formula unit and the unit cell volume. τj or τp represents the particle absorption factor for phase j and p.

The GSA was used to conduct surface area and porosity measurements. The tube was degassed at 300°C for 3 hours, then weighed and inserted into the micrometrics port. Analysis was carried out with liquid nitrogen as a probe molecule. BET and t-plot methods were used to measure specific surface area, micropore surface area, outer surface area, total pore volume,

and average pore radius. These measurements are based on isotherm adsorption data, which involves a monolayer of molecules on the adsorbent surface. The data obtained are changes in pressure (P/Po) and volume of N_2 gas(Buttersack et al., 2016; Naderi, 2015; Tran et al., 2018).

The NH_3-TPD instrument was used to determine the acidity of the Ni/HZSM-5 catalyst at different metal/support ratios. NH_3-TPD analysis entails heating the sample to 350°C for 60 minutes using a stream of helium gas. Ammonia adsorption (5% in He) was performed at 100°C for 30 minutes, followed by 30 minutes of washing with He. NH_3-TPD was then heated to 100-700°C at 10 °C/min and maintained for 10 minutes at 700°C. The NH_3 desorption peak area was determined using the TCD signal to estimate the sample's acidity. The number of acid sites is calculated by measuring the ammonia molecules adsorbed on the sample (Zhang et al., 2018). The NH_3 desorption peak at low temperatures is often induced by adsorbed Lewis acid sites, while the peak at 400-500°C is caused by adsorbed Brønsted acid sites (Chen et al., 2018; Chen et al., 2019; Nugrahaningtyas et al., 2024).

Catalytic Performance Test

The catalyst was formed into 0.5-gram pellets and heated at 110°C for 3 hours. The catalyst is placed in the reactor and heated to 400 ºC with H_2 flowing at a 5 mL/minute rate. Figure S1 (supplementary file) shows a schematic of the reactor. Anisole was introduced into the feed reactor in the following stage and purged with H_2 for 5 minutes. The feed reactor was heated to 155 ºC, with an H2 gas flow rate of 15 mL/min. The acquired products were examined with GC-MS to determine the type and quantity of the product. The percentage of total yield, conversion, and product selectivity were estimated using modified formulas from earlier studies (El-Hakam et al., 2013; Nugrahaningtyas et al., 2019; Choo et al., 2020; Yusuf et al., 2023). The formulas below were used to calculate the anisole conversion rate ($X_{anisole}$), product yield (Y_i), and selectivity (S_i).

$$X_{anisole}\ (wt\%) = \frac{weight\ of\ anisole\ consumed}{weight\ of\ anisole\ in\ feed} \times 100$$

Since one mol of anisole will only produce one mol of benzene, toluene or xylene.

$$Y_i(wt\%) = \frac{obtained\ weight\ of\ product\ i}{weight\ of\ anisole\ in\ feed} \times 100$$

$$S_i(\%) = \frac{weight\ of\ product\ i}{weight\ of\ anisole\ consumed} \times 100\%$$

RESULT AND DISCUSSION

Morphological Analysis

Figure 1 shows the morphological analysis results for samples at 5,000x and 50,000x magnification. The catalysts identified had irregular shapes and variable particle sizes. These findings follow previous research stating that adding metal did not change the shape of HZSM-5 (Niu et al., 2014). When metal is added, the surface and form of the Ni/HZSM-5 catalysts become heterogeneous relative to the support (HZSM-5). The appearance of a shining white stain after adding metal indicates Ni is impregnated.

Diffraction Pattern Analysis

The diffraction patterns of HZSM-5 and Ni/HZSM-5 are similar (**Figure 2**). The typical peak of Ni is not visible in **Figure 2**, indicating that Ni is evenly dispersed in HZSM-5(Niu et al., 2014). The addition of Ni is found to have a slight influence on the diffraction pattern of HZSM-5. The peaks that have undergone specific changes have been marked with an asterisk (*). The characteristic peak intensity of the material decreases slightly, suggesting an altered behavior of the material due to the presence of Ni. The refinement analysis also supports the results of the diffraction pattern analysis.

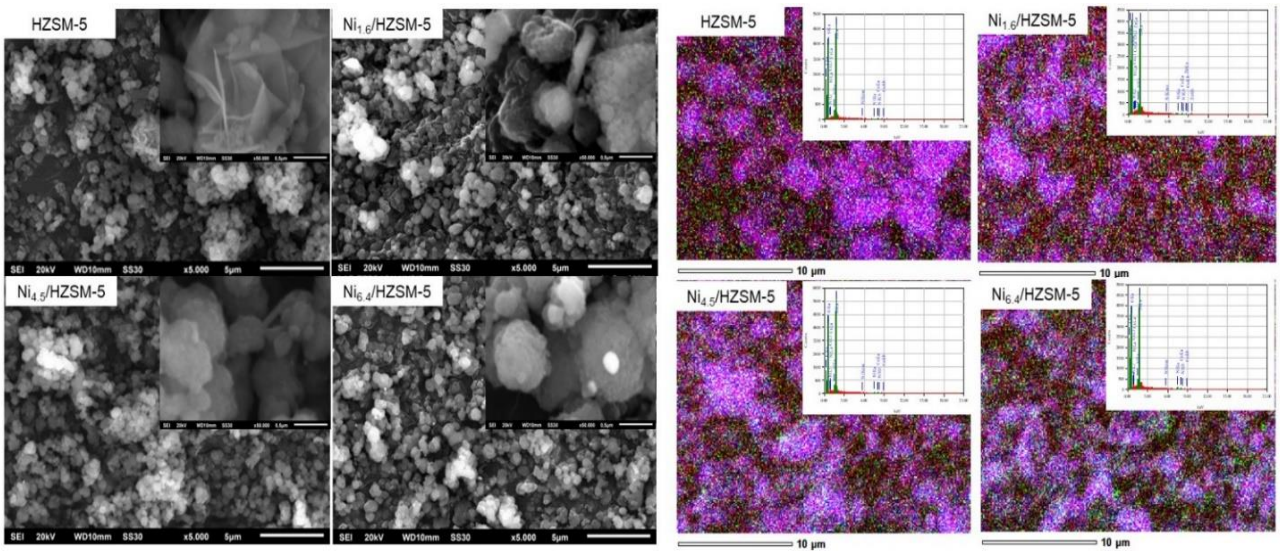

Figure 1. Morphology and element mapping for HZSM-5, $Ni_{1.6}$/HZSM-5, $Ni_{4.5}$/HZSM-5, and $Ni_{6.4}$/HZSM-5.

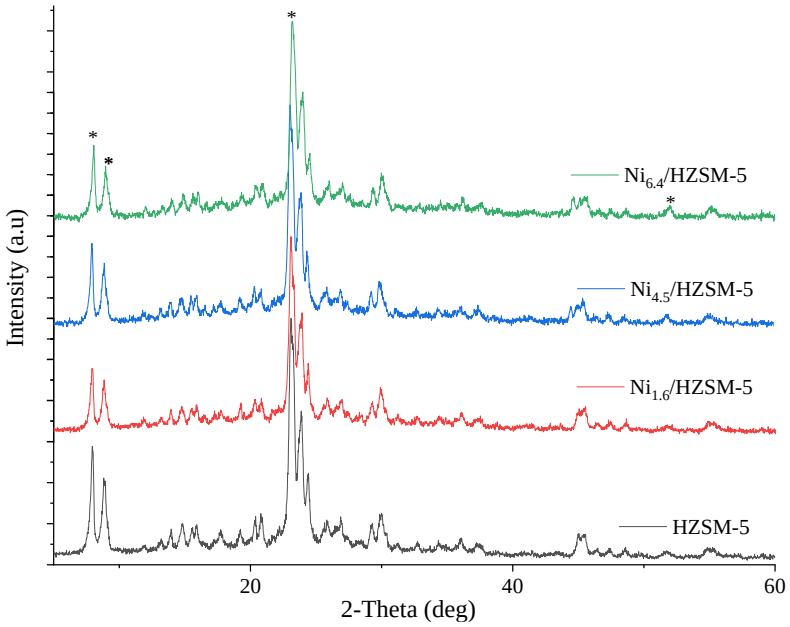

Figure 2. Diffraction patterns of the HZSM-5, $Ni_{1.6}$/HZSM-5, $Ni_{4.5}$/HZSM-5, and $Ni_{6.4}$/HZSM-5.

Table 1. Refinement results using HZSM-5 standard (ICSD #61010).

Cell Parameters	HZSM-5	$Ni_{1.6}$/HZSM-5	$Ni_{4.5}$/HZSM-5	$Ni_{6.4}$/HZSM-5
Crystal Structure	Orthorhombic	Orthorhombic	Orthorhombic	Orthorhombic
Space Group	P n 21 a	P n 21 a	P n 21 a	P n 21 a
a (Å)	20.16	20.21	20.25	20.15
b (Å)	19.93	19.95	19.97	19.89
c (Å)	13.38	13.39	13.41	13.35
angles (o)	α=β=γ=90	α=β=γ=90	α=β=γ=90	α=β=γ=90
Cell Volume (Å3)	5381.91	5399.85	5428.29	5354.90
Z	1	1	1	1
Rp (%)	5.67	5.62	5.05	5.04
Rwp (%)	5.47	6.08	5.00	5.41

Table 2. The molar weight percentage of the metal phase on the catalyst

Phase (ICSD #)	Molar Weight Percentage (%)		
	$Ni_{1.6}$/HZSM-5	$Ni_{4.5}$/HZSM-5	$Ni_{6.4}$/HZSM-5
HZSM-5 (#61010)	91.82	92.15	92.03
Ni (#53807)	2.99	3.04	3.00
NiO (#24014)	5.19	4.81	4.97

Refinement analysis is also used to determine the metal phase in the catalyst (**Table 2**). The refinement results show that metal oxides are more dominant than the metal element phase(Zheng et al., 2020).

Based on the residual factor values (Rp and Rwp), evaluate the appropriateness of the HZSM-5 standards (**Table 1**). The residual factor values decrease if the phases match the XRD pattern. The residual factor values (Rp and Rwp) were 5.67% and 5.47%, respectively. It demonstrates that the HZSM-5 employed met the HZSM-5 criteria (ICSD #61010). Apart from that, it is also known that the diffraction pattern of HZSM-5 is similar, but there is a slight decrease in the characteristic peak intensity of HZSM-5, which is thought to be due to the influence of the addition of Ni.

Catalyst Porosity

Overall, the surface area of HZSM-5 increases after the addition of metals (**Figure 3**). When metals are added to a support, and the surface area of the support increases, it suggests that the addition of metals doesn't lead to the accumulation of metals on the support surface or blockage of the pores by metals. Instead, the increase in specific surface area indicates that the metal has been evenly dispersed across the entire support surface, which allows the catalyst to activate more reactants and produce a greater amount of products. Meanwhile, the Ni/HZSM-5

catalyst exhibits a smaller micropore surface area compared to HZSM-5. Therefore, it is suspected that the addition of metals leads to the closure of some micropores. The increase in outer surface area indicates that nickel metal is bound to the outer surface of HZSM-5. Adding nickel metal, which supplies new active sites, helps reduce the loss of catalytic activity with a decrease in surface area(Zheng et al., 2020). Meanwhile, the average pore size and pore volume values tend to increase after the impregnation of Ni into HZSM-5. An increase in the average pore size indicates that the presence of metal causes the formation of new pores with a larger size(Trisunaryanti et al., 2010). In addition, calcination and reduction can open the pores of each catalyst, thereby increasing its volume. The adsorption isotherm graph data with the N_2 gas molecule probe also supports the surface area characteristics of the catalyst (**Figure 4**).

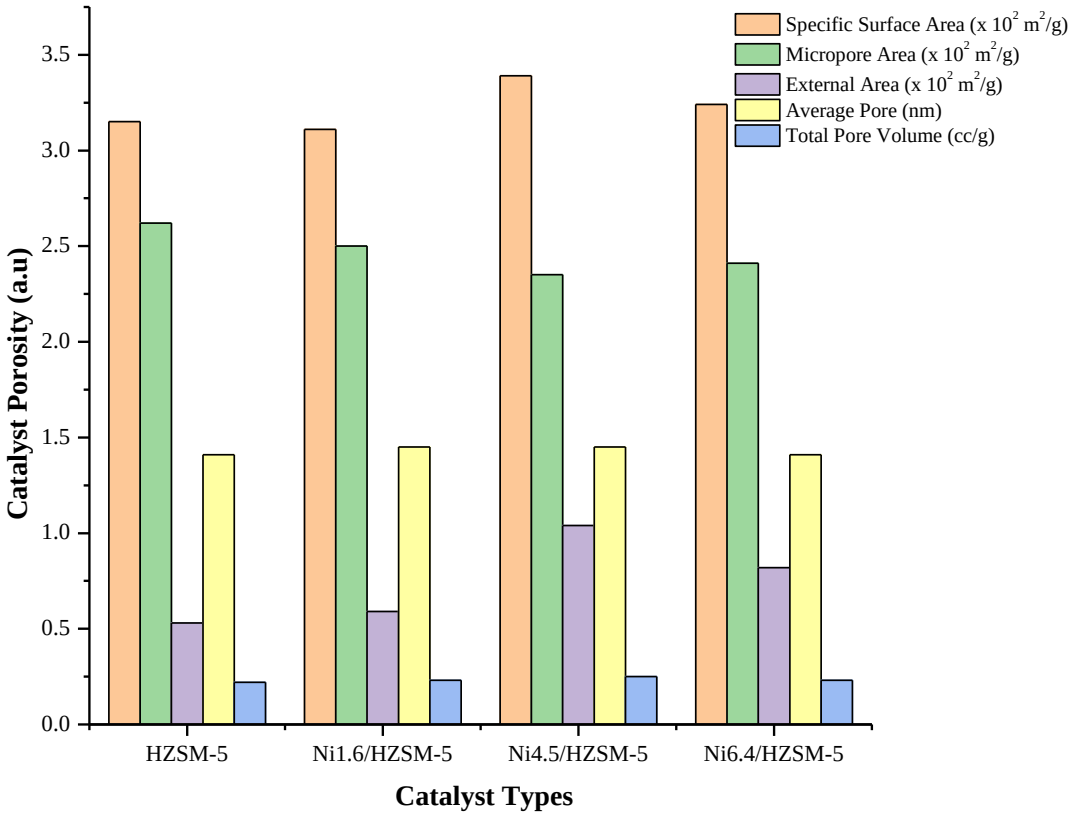

Figure 3. Surface area and porosity of $Ni_{1.6}$/HZSM-5, $Ni_{4.5}$/HZSM-5, and $Ni_{6.4}$/HZSM-5 catalyst.

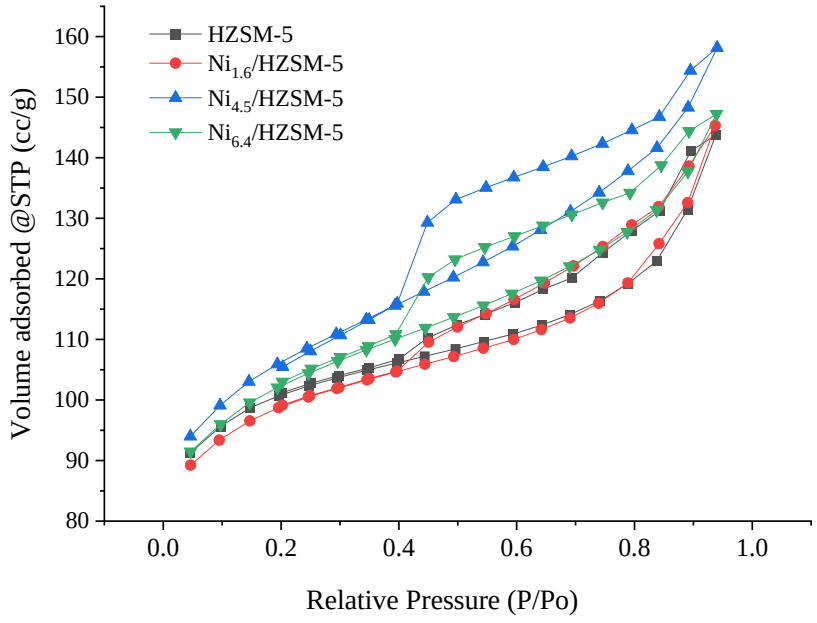

Figure 4. Adsorption-desorption isotherm graph of N_2 gas on catalyst.

Isotherm adsorption data can be utilized to characterize gas adsorption properties in porous materials (Pérez-Page et al., 2016; Sing, 2001). ZSM-5 possesses both micro and mesopores(Zhang et al., 2023). In this study, mesoporous ZSM-5 was utilized, as documented in the previous research. The N_2 adsorption-desorption isotherm graph resembles a type IV adsorption, it's a characteristic of mesoporous materials (2–50 nm, or 0.002-0.05 μm) (Bardestani et al., 2019). This statement agrees with the research data, as documented in the previous research (Ediati et al., 2017; Che et al., 2019; Zhao et al., 2019; Eschenbacher et al., 2020; Munir and Usman, 2022). Mesoporous materials show potent catalytic activity in the HDO anisole reaction because the pore diameter is suitable for anisole molecules to diffuse (Arun et al., 2015; Crawford et al., 2020).

Acidity Analysis

Ammonia desorption in TPD analysis was performed in stages at 100–850 °C temperatures (Fig 5a). Ammonia desorption peaks at low temperatures indicate ammonia adsorbed on weakly acidic sites, while desorption peaks at high temperatures indicate ammonia adsorbed on stronger acid sites. Adding metal to HZSM-5 reduces its total acidity value due to metal dispersion on its surface, inhibiting the NH_3 gas bound to its pores (Azreena et al., 2021). The support has a greater total acidity because metal does not cover the zeolite pores. Based on the amount of acid strength, each catalyst tends to have a dominant amount of weak acid strength, which shows that each catalyst has more Lewis acid sites than the Bronsted catalyst. Meanwhile, the low total acidity of Ni/HZSM-5 is thought to be because a Lewis acid site from the metal has replaced the Bronsted acid site (**Figure 5b**). The presence of the Lewis acid site is indicated by the ammonia desorption peak at low temperatures(Al-dughaither et al., 2014; Zheng et al., 2020).

Catalytic Activity

Catalytic activity can be assessed based on the total anisole conversion (**Figure 6**). The catalyst's dual function, deriving from both the Bronsted acid site of the support and the active site of the metal, suggests that the addition of metal could potentially enhance the conversion reaction. The metal aids in both the isomerization and hydrogenation processes. For instance, $Ni_{4.5}$/HZSM-5 exhibits a maximum conversion of 31.63%, attributed to its larger surface area and acidity. This enhanced surface area and acidity facilitate better access for reactants to reach the active site (Shim et al., 2015). Conversely, $Ni_{6.5}$/HZSM-5 demonstrates the lowest conversion compared to the other catalysts, possibly due to the absence of high acidity alongside the metal content and large surface area. Thus, it's strongly suspected that not all high surface areas are catalytically active. In the HDO anisole reaction, the acid site serves as the active site(Wang et al., 2010).

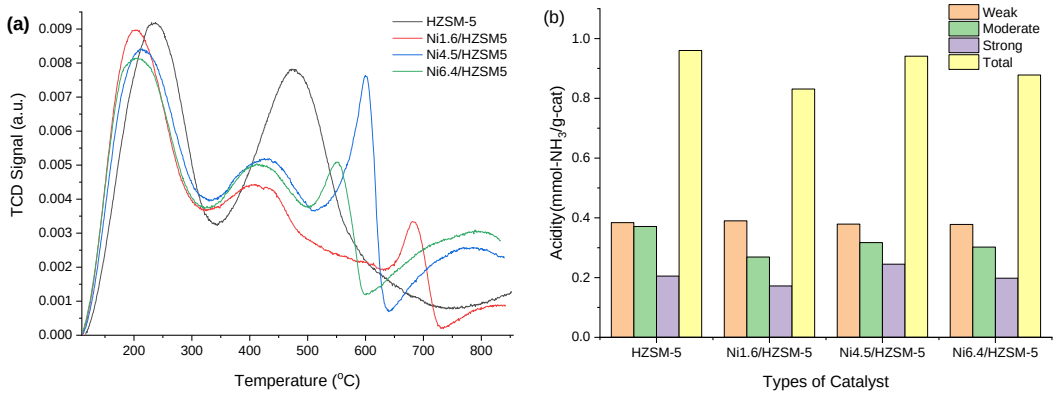

Figure 5. (a) Acid strength profile and (b) Acidity value of catalyst.

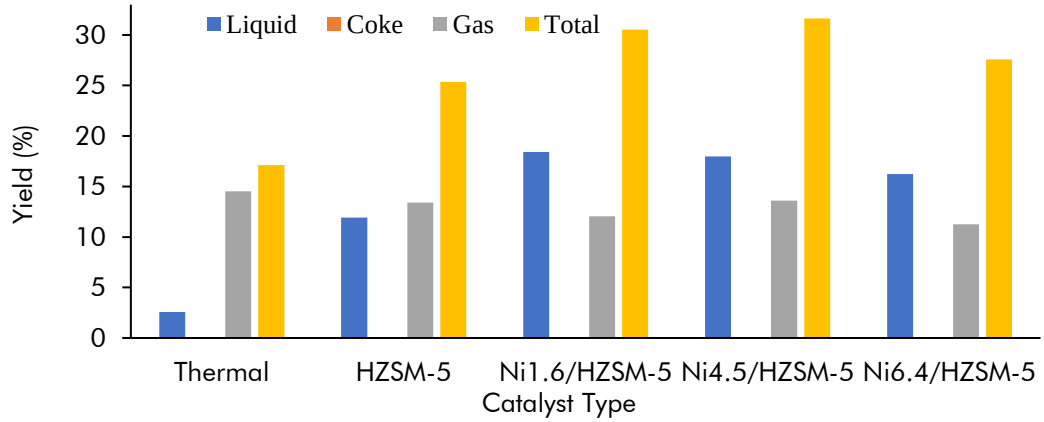

Figure 6. Product yield as a function of catalyst metal ratio.

The use of catalysts and the addition of metal can also increase the liquid products due to the increased pore volume after the addition of Ni. This facilitates the entry of anisole molecules into the catalyst pores, promoting increased interaction among them. This aids in anisole molecules entering the catalyst pores, enhancing their interaction. Furthermore, during the anisole HDO reaction, coke forms from heavy product condensation(Cardó et al., 2012), while anisole conversion produces gas, releasing oxygen as CO gas (Arun et al., 2015).

The liquid yield resulting from anisole conversion can be grouped into two groups, BTX compounds and compounds that still contain oxygen, including alcohols and aldehydes (intermediate compounds). Based on product analysis using GC-MS, each catalyst produces a different amount of product. However, the number of products yielded cannot be used as a reference for determining the best catalytic activity because the catalytic activity is assessed based on the total yield obtained. The product distribution of HDO anisole conversion compounds can be seen in **Table 3**.

The anisole hydrodeoxygenation mechanism involves demethylation or transmethylation, followed by hydrogenolysis. In catalysts, nickel serves as a hydrogen gas dissociator, with the first hydrogen atom binding to nickel and subsequent hydrogen atoms binding to methyl groups to form methane (CH_4). Anisole demethylation yields phenol as an intermediate, which is then hydrogenolyzed to produce benzene (Peters et al., 2015).

Toluene and xylene are produced from the transmethylation reaction in anisole by removing the -OH group. Toluene is produced from the cresol compound in a hydrodeoxygenation reaction which is accompanied by the release of water molecules, while xylene is produced from the hydrodeoxygenation reaction in methyl benzene (Ranga et al., 2018). Phenol is produced together with methyl benzene due to the release of several methyl groups attached to Ni, which are then bound back into anisole compounds that have not been completely converted. Additionally, transmethylation produces a side product called methyl anisole (Oyedun et al., 2019). No methylbenzene is produced because it may have been completely converted to xylene by a transmethylation reaction followed by hydrogenolysis.

Based on **Table 3**, it can be seen that the reactions that may occur during the anisole HDO process to form products include demethylation, transmethylation, and hydrogenolysis. The mechanism of the HDO reaction begins with H_2 being adsorbed and activated on the metal site, whereas oxygenate compounds can be adsorbed and activated on the metal site or on the impregnating agent (**Figure 7**). The hydrogen atom adsorbed on the Ni metal site will react with the adsorbed oxygenate compounds, causing the C-O bonds to be broken and the formation of deoxygenated products. The OH acid site interacts with the oxygen atom of the oxygenate compound and H_2 will be reactivated by the metal.

Table 3. Distribution of the HDO anisole product compound

Product compound	Yield (%)				
	Thermal	HZSM-5	$Ni_{1.6}$/HZSM-5	$Ni_{4.5}$/HZSM-5	$Ni_{6.4}$/HZSM-5
Benzene (C_6H_6)	0.752	0.268	0.246	0.457	0.469
Toluene (C_7H_8)	0.059	0.562	0.624	0.881	0.957
Xylene (C_8H_{10})	n.a	0.155	0.404	0.535	0.709
Naphthalene ($C_{10}H_8$)	n.a	n.a	0.219	n.a	n.a
Cresol (C_7H_8O)	n.a	2.916	2.847	3.290	2.766
Phenol (C_6H_6O)	0.983	6.352	8.781	10.647	9.353
Benzaldehyde (C_7H_6O)	0.786	n.a	0.683	n.a	0.159
Methyl anisole ($C_8H_{10}O$)	n.a	1.653	2.206	1.614	1.826

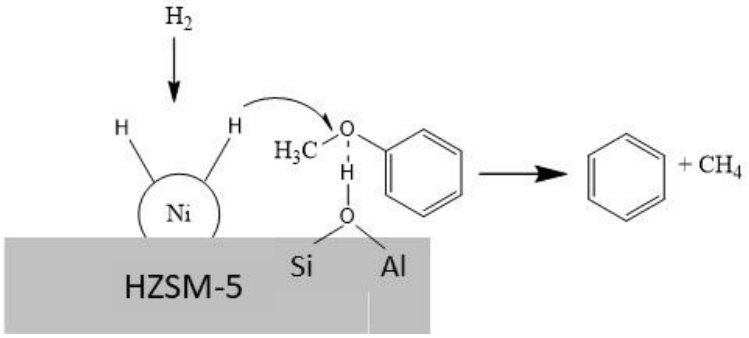

Figure 7. Proposed reaction mechanism for HDO anisole with Ni/HZSM-5 catalyst

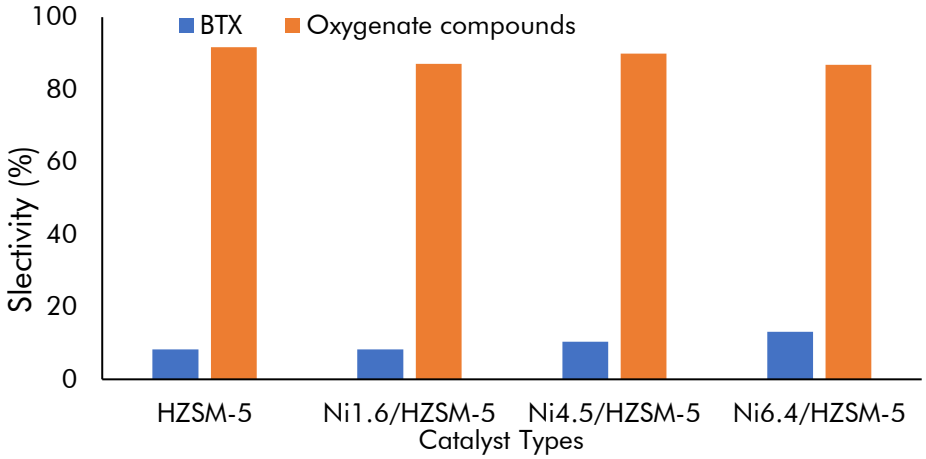

Figure 8. Product selectivity of various catalysts (a) BTX and (b) Oxygenate compounds.

Catalyst Selectivity

The use of the catalysts in this study resulted in different levels of selectivity against BTX (Figure 8). The addition of Ni to HZSM-5 increases the selectivity against BTX. The more metal contained, the higher the selectivity value. $Ni_{6.4}$/HZSM-5 has the highest amount of Ni compared to the other ones so that it produces the highest selectivity against BTX.

Pore size and acidity characteristics determine how anisole interacts with the catalyst, influencing the activation of anisole bonds. Anisole can adsorb onto the catalyst surface in three orientations: via epoxy oxygen, through the benzene ring horizontally, or vertically. Each orientation affects the activation of epoxy groups and phi bonds within the anisole, leading to variations in the catalyst properties that influence the range of anisole HDO products.

BTX are oxygen-free compounds which indicate the effectiveness of the anisole HDO reaction. They can be formed through several reaction routes, including direct deoxygenation and transalkylation-deoxygenation stepwise reactions(Asadieraghi et al., 2014; Gollakota et al., 2016; Gonalez-Borja & Resasco, 2011; Zhu et al., 2010). Acidic catalysts such as zeolites tend to show the gradual route of anisole hydrodeoxygenation(Gonalez-Borja & Resasco, 2011; Rogers & Zheng, 2016). The activation of the epoxy groups of anisole on the catalyst surface is not strong enough to release the oxygen bound to its benzene ring. As compensation, anisole is converted into phenol, leaving behind oxygenate compounds. Figure 8 presents the catalyst selectivity against products that still contain oxygen that are dominated by phenolic compounds. The phenolic products obtained are in accordance with the previous statement that the anisole hydrodeoxygenation reaction occurs in stages. Those are formed by a transmethylation reaction between two or more anisoles.

CONCLUSIONS

Based on the findings of this research, it is evident that the incorporation of Ni onto HZSM-5 was successfully accomplished, as confirmed by the presence of Ni on HZSM-5 according to EDS analysis. It was found that the structure of HZSM-5 was not affected by the addition of Ni, as there was no significant decrease in peak intensity in the XRD spectra of all catalysts. However, the addition of Ni increased the surface area and total pore volume, while decreasing the total acid strength of the catalysts. As a result, the application of Ni/HZSM-5 increased the activity and selectivity of the anisole HDO reaction. The highest activity was observed in $Ni_{4.5}$/HZSM-5, exhibiting the highest total anisole conversion, while the highest BTX selectivity was observed in $Ni_{6.4}$/HZSM-5.

ACKNOWLEDGMENTS

The author would like to thank Sebelas Maret University for funding this research through Hibah Grup riset (Penelitian HGR-UNS) A with contract number 228/UN27.22/PT.01.03/2023.

CONFLICT OF INTEREST

There is no conflict of interest with all coauthors

A DATA AVAILABILITY STATEMENT

All the data that support this study will be shared upon reasonable request to the corresponding author.

REFERENCES

Al-dughaither, A. S., de Lasa, H., & Lasa, H. De. (2014). HZSM-5 zeolites with different SiO_2 Al_2O_3 ratios. Characterization and NH_3 desorption kinetics. *Industrial & Engineering Chemistry Research, 53*(40), 15303–15316.

Arun, N., Sharma, R. V., & Dalai, A. K. (2015). Green diesel synthesis by hydrodeoxygenation of bio-based feedstocks: Strategies for catalyst design and development. *Renewable and Sustainable Energy Reviews, 48*, 240–255.

Asadieraghi, M., Wan Daud, W. M. A., & Abbas, H. F. (2014). Model compound approach to design process and select catalysts for in-situ bio-oil upgrading. *Renewable and Sustainable Energy Reviews, 36*, 286–303.

Bardestani, R., Patience, G. S., & Kaliaguine, S. (2019). Experimental methods in chemical engineering: specific surface area and pore size distribution measurements—BET, BJH, and DFT. *The Canadian Journal of Chemical Engineering, 97*(11), 2781–2791.

Botas, J. A., Serrano, D. P., García, A., De Vicente, J., & Ramos, R. (2012). Catalytic conversion of rapeseed oil into raw chemicals and fuels over Ni- and Mo-modified nanocrystalline ZSM-5 zeolite. *Catalysis Today, 195*(1), 59–70.

Buttersack, C., Möllmer, J., Hofmann, J., & Gläser, R. (2016). Determination of micropore volume and external surface of zeolites. *Microporous and Mesoporous Materials, 236*, 63–70.

Buzetzki, E., Sidorová, K., Cvengrošová, Z., & Cvengroš, J. (2011). Catalytic role of lignocellulosic materials in triacylglycerol cracking. *Journal of Analytical and Applied Pyrolysis, 92*, 314–323.

Cardó, X., Bergadà, O., Cesteros, Y., & Salagre, P. (2012). Effect of catalyst acidity and porosity on the catalytic isomerization of linoleic acid to obtain conjugated linoleic acids (CLAs). *Chemical Engineering Journal, 183*, 459–465.

Che, Q., Yang, M., Wang, X., Yang, Q., Chen, Y., Chen, X., Chen, W., Hu, J., Zheng, K., Yang, H., & Chen, H. (2019). Preparation of mesoporous ZSM-5 catalysts using green templates and their performance in biomass catalytic pyrolysis. *Bioresource Technology, 289*, 121729.

Chen, K., Zhang, T., Chen, X., He, Y., & Liang, X. (2018). Model construction of micro-pores in shale: A case study of Silurian Longmaxi Formation shale in Dianqianbei area, SW China. *Petroleum Exploration and Development, 45*(3), 412–421.

Chen, L., Janssens, T. V. W., Skoglundh, M., & Grönbeck, H. (2019). Interpretation of NH_3-TPD profiles from Cu-CHA using first-principles calculations. *Topics in Catalysis, 62*, 93–99.

Choo, M. Y., Oi, L. E., Ling, T. C., Ng, E. P., Lin, Y. C., Centi, G., & Juan, J. C. (2020). Deoxygenation of triolein to green diesel in the H_2-free condition: Effect of transition metal oxide supported on zeolite Y. *Journal of Analytical and Applied Pyrolysis, 147*, 104797, 1-8.

Crawford, J. M., Zaccarine, S. F., Kovach, N. C., Smoljan, C. S., Lucero, J., Trewyn, B. G., Pylypenko, S., & Carreon, M. A. (2020). Decarboxylation of stearic acid over Ni/MOR catalysts. *Journal of Chemical Technology & Biotechnology, 95*(1), 102–110.

Ediati, R., Mukminin, A., & Widiastuti, N. (2017). Impregnation of nickel on mesoporous ZSM-5 templated carbons as candidate material for hydrogen storage. *Indonesian Journal of Chemistry, 17*(1), 30–36.

El-Hakam, S. A., Samra, S. E., El-Dafrawy, S. M., Ibrahim, A. A., & Salama, R. S. (2013). Surface acidity and catalytic activity of sulfated titania supported on mesoporous MCM-41. *International Journal of Modern Chemistry, 5*(1), 55–70.

Eschenbacher, A., Goodarzi, F., Saraeian, A., Kegnaes, S., Shanks, B. H., Jensen, A. D., & Jensen, A. D. (2020). Performance of mesoporous HZSM-5 and Silicalite-1 coated mesoporous HZSM-5 catalysts for deoxygenation of straw fast pyrolysis vapors. *Journal of Analytical and Applied Pyrolysis, 145*, 104712.

Gamliel, D. P., Baillie, B. P., Augustine, E., Hall, J., Bollas, G. M., & Valla, J. A. (2018). Nickel impregnated mesoporous USY zeolites for hydrodeoxygenation of anisole. *Microporous and Mesoporous Materials, 261*, 18–28.

Gollakota, A. R. K. K., Reddy, M., Subramanyam, M. D., & Kishore, N. (2016). A review on the upgradation techniques of pyrolysis oil. *Renewable and Sustainable Energy Reviews, 58*, 1543–1568.

Gonalez-Borja, M. A., & Resasco, D. E. (2011). Anisole and guaiacol hydrodeoxygenation over monolithic Pt-Sn catalysts. *Energy and Fuels, 25*, 4155–4162.

He, Z., & Wang, X. (2013). Hydrodeoxygenation of model compounds and catalytic systems for pyrolysis bio-oils upgrading. *Catalysis for Sustainable Energy, 1*, 28–52.

Azreena, I. N., Lau, H. L. N. L. N., Asikin-Mijan, N., Hassan, M. A. A., Izham, S. M., Kennedy, E., Stockenhuber, M., Mastuli, M.S. S., Alharthi, F. A., Alghamdi, A. A., & Taufiq-Yap, Y. H. H. (2021). A promoter effect on hydrodeoxygenation reactions of oleic acid by zeolite beta catalysts. *Journal of Analytical and Applied Pyrolysis, 155*, 105044.

Jin, S., Xiao, Z., Li, C., Chen, X., Wang, L., Xing, J., Li, W., & Liang, C. (2014). Catalytic hydrodeoxygenation of anisole as lignin model compound over supported nickel catalysts. *Catalysis Today, 234*, 125–132.

Li, W., Li, F., Wang, H., Liao, M., Li, P., Zheng, J., Tu, C., & Li, R. (2020). Hierarchical mesoporous ZSM-5 supported nickel catalyst for the catalytic hydrodeoxygenation of anisole to cyclohexane. *Molecular Catalysis*, *480*, 110642, 1-8.

Li, Y., Zhang, C., Liu, Y., Tang, S., Chen, G., Zhang, R., & Tang, X. (2017). Coke formation on the surface of Ni/HZSM-5 and Ni-Cu/HZSM-5 catalysts during bio-oil hydrodeoxygenation. *Fuel, 189*, 23–31.

Mazlan, Nugrahaningtyas, K. D., & Rahmawati, F. (2022). Effect of Fe metal loading on the character of HZSM-5. In *AIP Conference Proceedings, 2391*(1), 050011. AIP Publishing

Munir, D., & Usman, M. R. (2022). Mesoporous HZSM-5 catalysts for the conversion of waste plastics to liquid fuels, *Journal of Porous Materials, 29*, 783–794.

Naderi, M. (2015). *Surface Area*: Brunauer-Emmett-Teller (BET). In S. Tarleton (Ed.), progress in filtration and separation. Cambridge: Academic Press.

Niu, X., Gao, J., Miao, Q., Dong, M., Wang, G., Fan, W., Qin, Z., & Wang, J. (2014). Influence of preparation method on the performance of Zn-containing HZSM-5 catalysts in methanol-to-aromatics. *Microporous and Mesoporous Materials, 197*, 252–261.

Nugrahaningtyas, K. D., Kurniawati, M. F., Masykur, A., & Quratul'aini, N.'A. (2022). Periodic trends in the character of first-row transition metals-based catalysts embedded on mordenite. *Moroccan Journal of Chemistry, 10*(3), 375–386.

Nugrahaningtyas, K. D., Rahmawati, N., Rahmawati, F., & Hidayat, Y. (2019). Synthesis and characterization of CoMo/mordenite catalyst for hydrotreatment of lignin compound Models. *Open Chemistry, 17*(1), 1061–1070.

Nugrahaningtyas, K. D., Sabiilagusti, A. I., Rahmawati, F., Heraldy, E., & Hidayat, Y. (2024). Hydrodeoxygenation of anisole via Cu supported on zeolite: HZSM-5, MOR, and Indonesian activated natural zeolite. *Ingeniería e Investigación, 44*(1), e106683.

Nugrahaningtyas, K. D., Suharbiansah, R. S. R., Lestari, W. W., & Rahmawati, F. (2022). Metal phase, electron density, textural properties, and catalytic activity of como based catalyst applied in hydrodeoxygenation of oleic acid. *Evergreen, 9*(2), 283–291.

Oyedun, A. O., Patel, M., Kumar, M., & Kumar, A. (2019). *Chemical Catalysts for biomass upgrading*, weinheim; Germany: Wiley-VCH Verlag GmbH & Co. KGaA.

Pérez-Page, M., Makel, J., Guan, K., Zhang, S., Tringe, J., Castro, R. H. R., & Stroeve, P. (2016). Gas adsorption properties of ZSM-5 zeolites heated to extreme temperatures. *Ceramics International, 42*(14), 15423–15431.

Peters, J. E., Carpenter, J. R., & Dayton, D. C. (2015). Anisole and guaiacol hydrodeoxygenation reaction pathways over selected catalysts. *Energy and Fuels, 29*(2), 909–916.

Rahimi, N., & Karimzadeh, R. (2011). Catalytic cracking of hydrocarbons over modified ZSM-5 zeolites to produce light olefins: A review. *Applied Catalysis A: General, 398*(1–2), 1–17.

Ranga, C., Alexiadis, V. I., Lauwaert, J., Lødeng, R., & Thybaut, J. W. (2019). Effect of Co incorporation and support selection on deoxygenation selectivity and stability of (Co)Mo catalysts in anisole HDO. *Applied Catalysis A: General, 571*, 61–70.

Ranga, C., Lødeng, R., Alexiadis, V. I., Rajkhowa, T., Bjørkan, H., Chytil, S., Svenum, I. H., Walmsley, J., Detavernier, C., Poleman, H., Van Der Voort, P., & Thybaut, J. W. (2018). Effect of composition and preparation of supported MoO_3 catalysts for anisole hydrodeoxygenation. *Chemical Engineering Journal, 335*, 120–132.

Rogers, K. A., & Zheng, Y. (2016). Selective deoxygenation of biomass-derived bio-oils within hydrogen-modest environments: A review and new insights. *ChemSusChem, 9*(14), 1750–1772.

Sabiilagusti, A. I., Nugrahaningtyas, K. D., & Hidayat, Y. (2021). Synthesis and metal phases characterization of mordenite supported copper catalysts. In *Journal of Physics: Conference Series*, *1912*(1), 012032. IOP Publishing.

Shim, J. O., Jeong, D. W., Jang, W. J., Jeon, K. W., Kim, S. H., Jeon, B. H., Roh, H.S., Na, J. G., Oh, Y. K., Han, S. S., & Ko, C. H. (2015). Optimization of unsupported CoMo catalysts for decarboxylation of oleic acid. *Catalysis Communications, 67*, 16–20.

Sing, K. (2001). The use of nitrogen adsorption for the characterisation of porous materials. *Colloids and Surfaces A: Physicochemical and Engineering Aspects, 187–188*, 3–9.

Tamer, M. (2013). quantitative phase analysis based on rietveld structure refinement for carbonate rocks. *Journal of Modern Physics, 04*(08), 1149–1157.

Toraya, H. (2016). A new method for quantitative phase analysis using X-ray powder diffraction: Direct derivation of weight fractions from observed integrated intensities and chemical compositions of individual phases. *Journal of Applied Crystallography, 49*(5), 1508–1516.

Tran, H. N., Lee, C. K., Nguyen, T. V., & Chao, H. P. (2018). Saccharide-derived microporous spherical biochar prepared from hydrothermal carbonization and different pyrolysis temperatures: synthesis, characterization, and application in water treatment. *Environmental Technology, 39*(21), 2747–2760.

Trisunaryanti, W., Triwahyuni, E., & Sudiono, S. (2010). Preparation, characterizations and modification of ni-pd/natural zeolite catalysts. *Indonesian Journal of Chemistry*, *5*(1), 48–53.

Venkatesan, K., Krishna, J. V. J., Anjana, S., Selvam, P., & Vinu, R. (2021). Hydrodeoxygenation kinetics of syringol, guaiacol and phenol over H-ZSM-5. *Catalysis Communications, 148*, 106164.

Wang, W., Yang, Y., Luo, H., & Liu, W. (2010). Characterization and hydrodeoxygenation properties of Co promoted Ni-Mo-B amorphous catalysts: influence of co content. reaction

kinetics, *Mechanisms and Catalysis, 101*(1), 105–115.

Will, G. (2006). *Powder diffraction*: The rietveld method and the twostage method to determine and refine crystal structures from powder diffraction data. Powder Diffraction: The Rietveld Method and the Two Stage Method to Determine and Refine Crystal Structures from Powder Diffraction Data. Berlin; Heidelberg: Springer-Verlag.

Yang, Y., Ochoa-Hernández, C., de la Peña O'Shea, V. A., Pizarro, P., Coronado, J. M., & Serrano, D. P. (2014). Effect of metal–support interaction on the selective hydrodeoxygenation of anisole to aromatics over Ni-based catalysts. *Applied Catalysis B: Environmental, 145*, 91–100.

Yusuf, M., Leeke, G., & Wood, J. (2023). Anisole hydrodeoxygenation over nickel-based catalysts: influences of solvent and support properties. *Energy and Fuels, 37*, 1225-1237.

Zhang, D., Zhao, Y. P., Fan, X., Liu, Z. Q., Wang, R. Y., & Wei, X. Y. (2018). Catalytic hydrogenation of levulinic acid into gamma-valerolactone over Ni/HZSM-5 catalysts. *Catalysis Surveys from Asia, 22*(3), 129–135.

Zhang, D., Jin, T., Peng, J., Ma, J., Zhang, J., Tian, X., & Ding, M. (2023). In-situ synthesis of micro/mesoporous HZSM-5 zeolite for catalytic pyrolysis of lignin to produce monocyclic aromatics. *Fuel, 334*, 126588.

Zhang, J., Fidalgo, B., Kolios, A., Shen, D., & Gu, S. (2018). Mechanism of deoxygenation in anisole decomposition over single-metal loaded HZSM-5: Experimental study. *Chemical Engineering Journal, 336*, 211–222.

Zhang, J., Fidalgo, B., Wagland, S., Shen, D., Zhang, X., & Gu, S. (2019). Deoxygenation in anisole decomposition over bimetallic catalysts supported on HZSM-5. *Fuel, 238*, 257–266.

Zhao, T., Li, F., Yu, H., Ding, S., Li, Z., Huang, X., Li, X., Wei, X., Wang, Z., Lin, H. (2019). Synthesis of mesoporous ZSM-5 zeolites and catalytic cracking of ethanol and oleic acid into light olefins. *Applied Catalysis A: General, 575*, 101–110.

Zheng, Y., Wang, J., Liu, C., Lu, Y., Lin, X., Li, W., & Zheng, Z. (2020). Efficient and stable Ni-Cu catalysts for ex situ catalytic pyrolysis vapor upgrading of oleic acid into hydrocarbon: Effect of catalyst support, process parameters and Ni-to-Cu mixed ratio. *Renewable Energy, 154,* 797–812.

Zhu, X., Mallinson, R. G., & Resasco, D. E. (2010). Role of transalkylation reactions in the conversion of anisole over HZSM-5. *Applied Catalysis A: General, 379*, 172–181.